

GaAs metal–semiconductor–metal photodetectors with low dark current and high responsivity at 850 nm

This content has been downloaded from IOPscience. Please scroll down to see the full text.

2002 Semicond. Sci. Technol. 17 1261

(<http://iopscience.iop.org/0268-1242/17/12/309>)

View [the table of contents for this issue](#), or go to the [journal homepage](#) for more

Download details:

IP Address: 140.113.38.11

This content was downloaded on 28/04/2014 at 03:56

Please note that [terms and conditions apply](#).

GaAs metal–semiconductor–metal photodetectors with low dark current and high responsivity at 850 nm

S D Lin and C P Lee

Department of Electronics Engineering, National Chiao Tung University,
1001 Ta Hsueh Road, Hsinchu, Taiwan, Republic of China

Received 29 August 2002, in final form 16 October 2002

Published 7 November 2002

Online at stacks.iop.org/SST/17/1261

Abstract

In this paper, we report on the fabrication a GaAs metal–semiconductor–metal photodetector with both low dark current and high responsivity at 850 nm. By using the Schottky contacts modified by a thin, n^+ -doped layer on the surface of the devices, the lowest dark current density of about $4.5 \times 10^{-7} \text{ cm}^{-2}$ was achieved. Besides, in the same devices, the responsivity resulting from a newly designed resonant-cavity-enhanced structure with a superlattice distributed Bragg reflector was about 0.34 A W^{-1} at 850 nm. The equivalent external quantum efficiency of the devices with equal finger spacing and finger width was about 48%. Our design is relatively easy and reproducible for both the sample growth and the device process.

1. Introduction

Low-noise and high-speed photodetectors are indispensable components for high-speed fibre communication systems and optical interconnection modules. It is well known that metal–semiconductor–metal photodetectors (MSMPDs) have several advantages [1–4] compared with traditional p–i–n photodiodes. Firstly, they have a planar structure, which is compatible with most electronic devices, making them ideal for optoelectronic integrated circuit (OEIC) applications. Secondly, because of their geometry, they have a lower capacitance for the same active area resulting in a lower (RC) time delay. Thirdly, the process for fabricating these devices is very simple and is compatible with regular IC processes. All of these properties make MSMPDs attractive for high-speed communication applications.

However, large dark current and poor responsivity remain as problem areas for MSMPDs in various applications. Because the dark current is normally controlled by the Schottky barrier of the metal contacts of the devices, there have been several methods developed to engineer the Schottky barrier height, including epitaxial structure adjustment and device process treatment [5–11]. However, to date, the lowest reported dark current densities for GaAs [5] and InGaAs [7] (on InP substrates, with an InAlAs Schottky barrier enhancement layer) MSMPDs are about $6 \times 10^{-6} \text{ cm}^{-2}$

and $2 \times 10^{-6} \text{ cm}^{-2}$, respectively. Most of these methods also rely on complicated and often difficult fabrication processes. There have also been several methods developed to enhance the responsivity of the devices [12–15]. From these, the transparent fingers and resonant-cavity-enhanced (RCE) structures are more effective than others. A transparent electrode, such as ultra-thin metal or indium–tin oxide (ITO) Schottky contacts, however, suffers from reliability and/or reproducibility problems. The RCE structure is a good solution for responsivity enhancement, because it uses a thin absorption layer and has an almost 100% internal quantum efficiency. Unfortunately, in conventional RCE designs, the tolerance of the layer thickness and/or the device process is relatively small. And most importantly, the compatibility with other devices, e.g. field-effect transistors (FETs), and/or processes has to be sacrificed.

To overcome these difficulties mentioned above, we have developed a GaAs MSMPD which has both low dark current and high responsivity at 850 nm. Our design is easy and reproducible for both the sample growth and the device process. By using the Schottky contacts modified by a thin, n^+ -layer on the surface, we achieved a reduction in the dark current of three orders of magnitude. The resulting dark current density was about $4.5 \times 10^{-7} \text{ cm}^{-2}$. This is the lowest dark current density for GaAs MSMPDs reported so far. Besides, in the same devices, we used a resonant cavity

to enhance the responsivity. The responsivity was about 0.34 A W^{-1} at 850 nm. The equivalent external quantum efficiency of the devices with equal finger spacing and finger width was about 48%. This means that almost all incident light through the spacing between the fingers was absorbed and converted into photocurrent.

2. Device structure design

2.1. Reduction of dark current with modified Schottky contacts

A conventional MSMPD consists of two back-to-back Schottky diodes. Based on Sze's work in 1971 [17], ignoring the two-dimensional and the image force lowering effects, under the flat-band condition, i.e. the semiconductor between two metal contacts totally depleted, the total current J_t through the structure can be described approximately by the simple relation

$$J_t = J_n + J_p = A_n^* T^2 e^{-q\phi_{bn}/kT} + A_p^* T^2 e^{-q\phi_{bp}/kT} \quad (1)$$

where J_n (J_p) is the electron (hole) current injected from the cathode (anode), ϕ_{bn} (ϕ_{bp}) is the electron (hole) Schottky barrier height, and A_n^* (A_p^*) is the effective Richardson's constant for the electron (hole). In a conventional, unmodified Schottky contact, the sum of the electron and the hole Schottky barrier heights equals the energy gap of the semiconductor, i.e.

$$\phi_{bn} + \phi_{bp} = E_g. \quad (2)$$

This relation has been proven by experiments on many semiconductors [18, 19]. From equations (1) and (2), it is obvious that, if we try to reduce the electron flow in the dark current, the hole current will increase at the same time, and vice versa. However, if the Schottky contact is modified, it is possible that the sum of ϕ_{bn} and ϕ_{bp} will be larger than E_g [16]. The dark current can then be reduced. For GaAs with a Ti/Pt/Au Schottky contact, the unmodified electron (hole) Schottky barrier height is about 0.8–0.85 eV (0.62–0.57 eV). So the dark current of GaAs MSMPDs is dominated by the hole current (J_p). In this work, we have used a thin, highly-doped n^+ surface layer to increase the hole Schottky barrier height. In this way, the hole conduction is suppressed while the electron current remains low.

We assume that the doping concentrations and the thickness of the thin n^+ layer are N_D and d , respectively. According to the depletion model, the enhancement of the hole Schottky barrier height ($\Delta\phi_{bp}$) is

$$\Delta\phi_{bp} = \frac{qN_D}{2\epsilon_s} d^2 \quad (3)$$

where q is the unit electron charge and ϵ_s is the dielectric constant of the semiconductor [18, 20]. In this study, the n^+ layer was chosen to be 15 nm thick with a doping concentration of $2 \times 10^{18} \text{ cm}^{-3}$. In this case, the dark current is still dominated by the hole current injected from the anode and, based on equation (3), the enhancement of the hole Schottky barrier height ($\Delta\phi_{bp}$) is about 0.31 eV. So, according to equation (1), we achieve a reduction in dark current of several orders of magnitude.

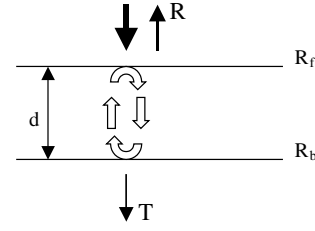


Figure 1. A schematic diagram of a RCE structure.

2.2. Enhancement of responsivity by RCE structure with a superlattice distributed Bragg reflector

For many years, it has been known that a resonant cavity can be used to enhance the quantum efficiency of a PD [21, 22]. In this work, we combine the resonant cavity design with our low dark current MSM structure. Detectors with very high quantum efficiency and a very low dark current were achieved. The device was designed in such a way that only one distributed Bragg reflector (DBR) was used. So the process is very simple and is compatible with that of conventional MSM detectors.

In a RCE PD, as shown schematically in figure 1, the quantum efficiency of the device is

$$\eta = 1 - T - R = (1 - R_f)(1 - e^{-\alpha d}) \times \frac{1 + R_b e^{-\alpha d}}{1 + R_\alpha^2 - 2R_\alpha \cos(4n_s \pi d/\lambda)} \quad (4)$$

where T and R are the transmittance and reflectance of the structure, respectively. R_f (R_b) is the reflectivity of the front (back) side interface, and R_α is defined to be $R_\alpha \equiv \sqrt{R_b R_f} \cdot e^{-\alpha d}$ [22]. The parameters α , d and n_s are the absorption coefficient, thickness and refractive index, respectively, and λ is the wavelength of the incident light. Under resonant condition, i.e.

$$d = m \frac{\lambda}{2n_s} \quad m = 1, 2, 3, \dots \quad (5)$$

the quantum efficiency is maximized. Furthermore, if the front mirror reflectivity, R_f , satisfies

$$R_f = R_b e^{-2\alpha d}$$

the quantum efficiency becomes the highest:

$$\eta_{\max} = (1 - e^{-\alpha d}) \frac{1 + R_b e^{-\alpha d}}{1 - R_b e^{-2\alpha d}}. \quad (6)$$

It is not difficult to see that, if $R_b \approx 1$, η_{\max} will be close to unity, which means that all the incident light is absorbed by the RCE structure. According to the above calculation, we can design the RCE MSMPD at 850 nm in the following way.

First, because a larger R_b gives higher quantum efficiency (η), we need a DBR with a high reflectivity at 850 nm. For semiconductor DBRs, $\text{Al}_y\text{Ga}_{1-y}\text{As}/\text{Al}_x\text{Ga}_{1-x}\text{As}$ ($y \sim 1$, $x \sim 0-0.3$) DBRs are commonly used and have been applied at the wavelength region from visible to near-infrared. In conventional 850 nm DBRs, in order to avoid the absorption of GaAs at 850 nm, we have to replace GaAs with $\text{Al}_x\text{Ga}_{1-x}\text{As}$ for the high refractive index layer, as shown in figure 2(a). However, in this way the refractive index difference is reduced, and the number of layers has to be increased for a certain reflectivity. In this work, we propose a new DBR structure to solve this difficulty. By using an AlAs/GaAs superlattice

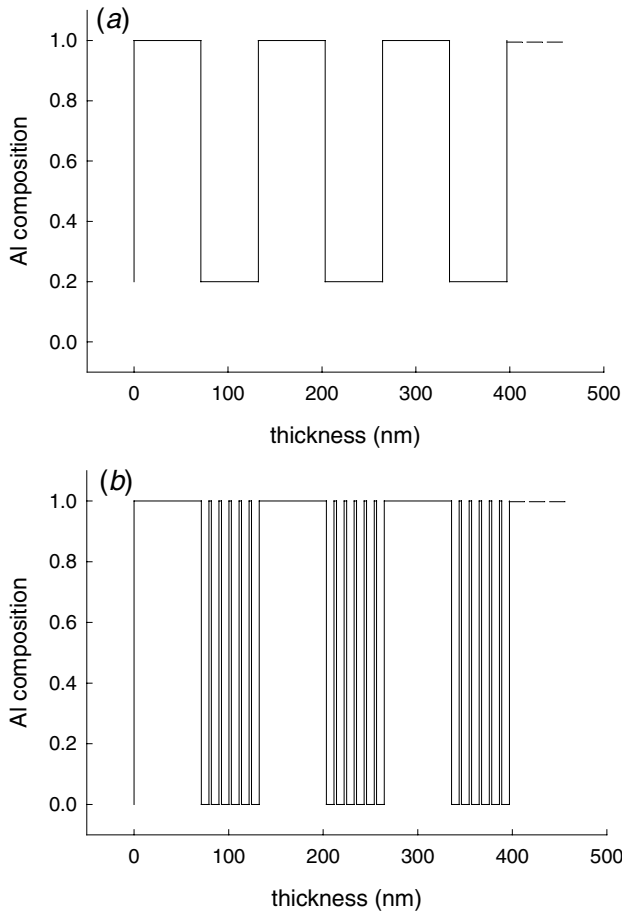


Figure 2. Structure diagrams of (a) a conventional AlAs/Al_{0.2}Ga_{0.8}As DBR and (b) an AlAs/GaAs SL-DBR.

for the high index regions, we can increase the bandgap of the region due to the quantum effect. Figure 2(b) shows the DBR structure used in this work. Under the constraint of a constant optical path length of a quarter wavelength, we can find suitable numbers and thicknesses of the AlAs and GaAs layers to avoid any absorption at 850 nm in the superlattice region. Our simple calculation result shows that five 2.5 nm AlAs layers in six 8 nm GaAs layers can keep the absorption edge at about 830 nm. Even if we take the two-dimensional (2D) exciton effect into consideration, this design should be sufficient to avoid any absorption at 850 nm [21]. Figure 3 shows the calculated reflectivity of the superlattice (SL) DBR at 850 nm as a function of the number of periods. For comparison, the calculated reflectivities of AlAs/GaAs and AlAs/Al_{0.2}Ga_{0.8}As DBRs are also shown in the figure. The absorption of GaAs at 850 nm is omitted in the calculation. The Al_{0.2}Ga_{0.8}As/AlAs DBR is included for comparison because the average Al composition of the superlattice is equal to 20%. From figure 3, we can see that, for a fixed number of periods, the reflectivity of the AlAs/Al_{0.2}Ga_{0.8}As DBR is lower than that of the AlAs/GaAs DBR as expected, because of a smaller difference of refractive index. However, the reflectivity of the SL-DBR is almost the same as that of the AlAs/GaAs DBR. The reason for the higher reflectivity in SL-DBRs can be understood as follows. For the same periods of DBRs, a larger difference of refraction index between the two materials gives

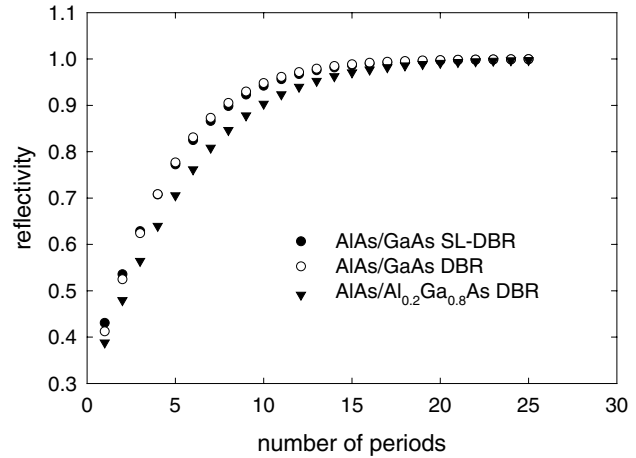


Figure 3. The calculated reflectivity at 850 nm as a function of the periods of high–low index pairs for the three types of DBR.

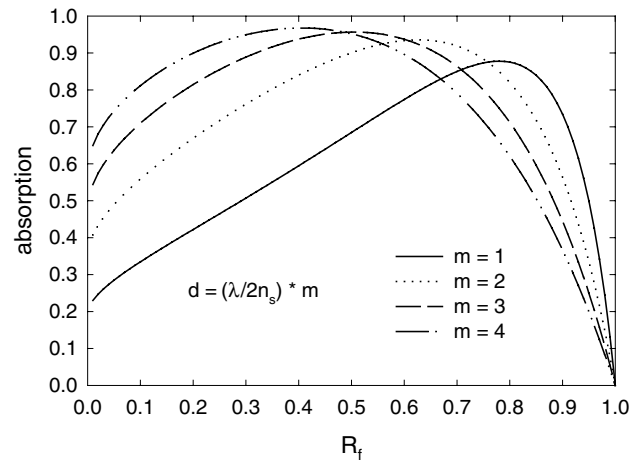


Figure 4. The calculated quantum efficiency of a RCE structure under different R_f for various absorption layer thicknesses in the resonant condition.

higher reflectivity. Compared with Al_{0.2}Ga_{0.8}As/AlAs DBRs, the AlAs/GaAs SL-DBRs have a larger index difference, so a higher reflectivity was obtained in the above-calculated result. It should be mentioned that another major advantage of this new DBR is that it does not absorb light at 850 nm.

We then consider the design of the front-mirror reflectivity (R_f) and the absorption layer thickness (d). Figure 4 shows the dependence of η on the front-side reflectivity R_f for different absorption layer thicknesses. R_b is fixed at 0.97 in the calculation, which can be achieved easily by a twelve-period SL-DBR mentioned above. From the figure, we can see that, when d equals four times the half-wavelength, we can obtain a very high absorption ($\approx 95\%$) for a large region of R_f around 0.35. Because the reflectivity of the GaAs/air interface is about 0.32 at 850 nm, the absorption thickness of four times the half-wavelength is suitable for our design of MSMPD.

Because of the need for passivation on the surface of GaAs MSMPDs, we have to consider the passivation layer effect on R_f . Figure 5 shows the relation between the thickness of the dielectric layer and front-side reflectivity R_f . From the figure, we can see that, even there is a $\pm 20\%$ thickness error during the deposition of the passivation layer, R_f is still in the region

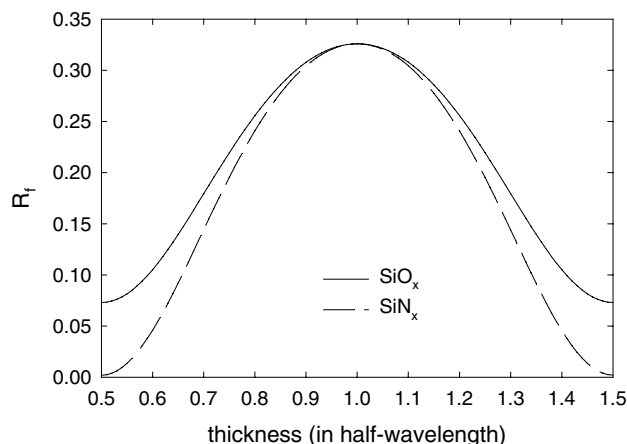


Figure 5. The calculated dependence of R_f on the thickness of the dielectric layer for SiO_x and SiN_x .

15 nm n^+ -GaAs
~450nm i-GaAs
12 periods AlAs/GaAs SL-DBR
Buffer GaAs
(100) S.I. GaAs substrate

Figure 6. The epitaxy structure of the RCE MSMPDs used in this study.

for almost maximum absorption ($\geq 90\%$). Therefore, from the above calculation, high quantum efficiency GaAs MSMPDs at 850 nm can be easily fabricated.

3. Sample growth and device fabrication

The samples used for this study were grown by molecular beam epitaxy using a Varian GEN II system. The sample structure is schematically shown in figure 6. Starting from the (100) semi-insulating GaAs substrate and the GaAs buffer layer, it consists of a twelve-period SL-DBR, a GaAs absorption layer with a thickness of four half-wavelengths at 850 nm, and a 15 nm n^+ -doped GaAs layer with a concentration of $2 \times 10^{18} \text{ cm}^{-3}$. All the layers except the top 15 nm GaAs layer were undoped. In order to minimize the effect of the dopant diffusion during growth, the substrate temperature was decreased from the normal growth temperature of 575 °C to about 540 °C before the top layer growth. Besides, to make sure that the grown structure meets the design criterion, another sample without an absorption layer was also grown for comparison.

Before device processing, the reflectivity of the samples was measured in advance. Figure 7(a) shows the reflectivity spectra of the sample without the absorption layer. From the figure, it is obvious that the sample without an absorption layer (i.e. SL-DBR only) has a very high reflectivity of about 0.97 at 850 nm as expected. The two dips at about 820 and 830 nm are due to the 2D exciton absorption in high-index SL layers. On the other hand, as shown in figure 7(b), the reflection spectrum of the sample with an absorption layer was also measured after chemical etching for different etching times, for matching the

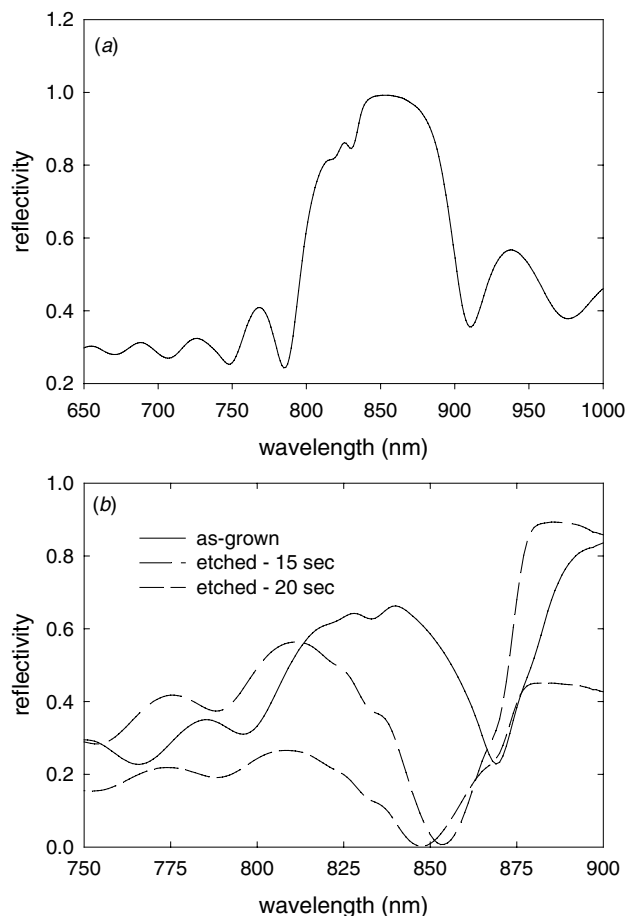


Figure 7. The measured reflectivity spectrum of the samples (a) without and (b) with an absorption layer.

cavity wavelength to 850 nm. Unlike the reflection spectrum shown in figure 7(a) (from the sample without an absorption layer), for the as-grown sample with an absorption layer, the dip in the reflection spectrum, or the highest absorption, occurs at about 870 nm (the solid line in figure 7(b)). This is because of the top n^+ layer. However, after a 15–20 s chemical etch in a solution of $\text{H}_3\text{PO}_4:\text{H}_2\text{O}_2:\text{H}_2\text{O}$ (3:1:50), the dip shifted to about 850 nm as designed (the two dashed lines in figure 7(b)).

After the above etching test, the MSMPD devices were fabricated. The MSMPDs were processed by a conventional method, consisting of three main steps: finger metallization, dielectric passivation and isolation, and pad formation. The surface n^+ layer not covered by the metal electrodes was etched away as described above using the finger metal as the mask. The Schottky metal used was Ti/Pt/Au, with a thickness of 30 nm/30 nm/100 nm. After both anode and cathode finger electrodes were formed, a surface passivation layer of 300 nm (half-wavelength of 850 nm) silicon oxide (SiO_x) was deposited using plasma-enhanced chemical vapour deposition (PECVD). A schematic diagram of the processed devices is shown in figure 8. In the finished devices, the finger spacing and width were both 6 μm , and the active area was $150 \times 150 \mu\text{m}^2$. For comparison, we have also processed a sample with the top n^+ layer removed to see the effect of the n^+ layer on the dark current.

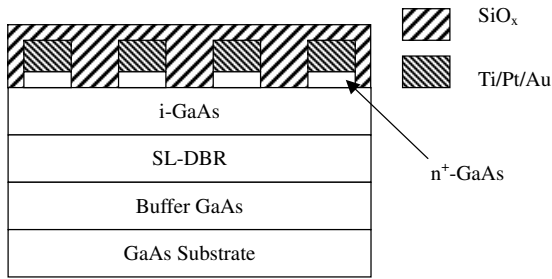


Figure 8. A schematic diagram of the structure of the processed MSMPDs.

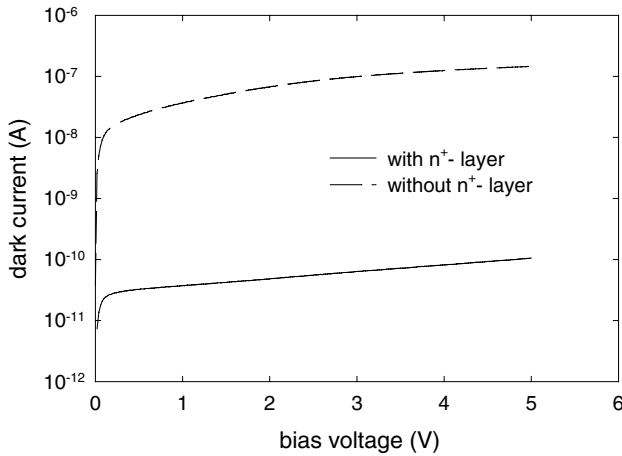


Figure 9. The measured dark current–voltage characteristics of the devices with and without the n^+ layer.

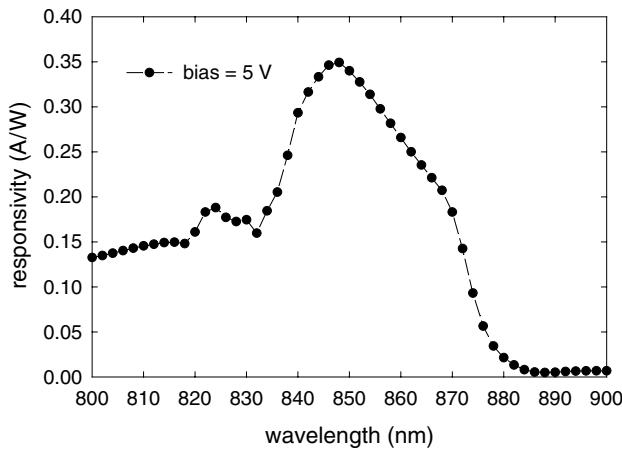


Figure 10. The measured responsivity spectrum of the MSMPD.

4. Result and discussion

The dark current characteristics of the devices were measured with an HP4145 semiconductor parameter analyser on a probe station. As shown in figure 9, the dark current of the devices is about 105 pA at a bias of 5 V. Compared with the dark current of the devices without the n^+ layer, the reduction of the dark current was over three orders of magnitude. The dark current density of the MSMPDs was about $4.5 \times 10^{-7} \text{ A cm}^{-2}$. To our knowledge, this is the lowest dark current density for GaAs MSMPDs reported so far.

After this, the responsivity of the devices was measured by a conventional lock-in method. Figure 10 shows the measured responsivity spectrum at a bias of 5 V. From the figure, we can see that the peak wavelength of the device is about 848 nm, which is in good agreement with the reflectivity result shown in figure 7(b). The responsivity at 850 nm and the corresponding external quantum efficiency (η_{ext}) are about 0.34 A W^{-1} and 48%, respectively. Because half of the incident light was blocked by the metal fingers, the η_{ext} of 48% means that the incident light through the spacing of the fingers was almost totally converted into the photocurrent.

5. Conclusion

In this work, GaAs MSMPDs with low dark currents and high responsivities at 850 nm have been designed and fabricated successfully. Using a Schottky contact modified with a 15 nm, $2 \times 10^{18} \text{ cm}^{-3}$ n^+ -doped surface layer, the dark current of MSMPDs can be suppressed by over three orders of magnitude compared with those of conventional ones. The dark current density of the devices was as low as $4.5 \times 10^{-7} \text{ cm}^{-2}$, which is the lowest dark current density for GaAs MSMPDs in reported results. Furthermore, to enhance the responsivity of the MSMPDs, we designed a RCE structure with a SL-DBR. In the designed RCE structure, the conditions of sample growth and device processing were considered carefully, making the device processing simple and reproducible. We consistently obtained fabricated devices with a responsivity of about 0.34 A W^{-1} at 850 nm. The equivalent external quantum efficiency of the devices was about 48%, which means almost all incident light through the spacing of the metal fingers was absorbed. Because of the relatively thin absorption layer, a good high-speed performance in the devices is expected.

Acknowledgments

This work was supported by the National Science Council under contract no NSC 90-2215-E-009-092 and the Lee-MTI Center of National Chiao Tung University.

References

- [1] Berger P R 1996 MSM photodiode *IEEE Potentials* **15** 25–9
- [2] Soole J B D and Schumacher H 1991 InGaAs metal–semiconductor–metal photodetectors for long wavelength optical communications *IEEE J. Quantum Electron.* **27** 737–52
- [3] Fay P, Wohlmuth W, Mahajan A, Caneau C, Chandrasekhar S and Adesida I 1998 A comparative study of integrated photoreceivers using MSM/HEMT and PIN/HEMT technologies *IEEE Photon. Technol. Lett.* **10** 582–4
- [4] Martin E A, Vaccaro K, Spaziani S M and Lorenzo J P 1995 Backside illumination processing technology for InGaAs/InAlAs/InP photofets and MSMs *Microelectron. J.* **26** 497–505
- [5] Ito M and Wada O 1986 Low dark current GaAs metal–semiconductor–metal (MSM) photodiodes using WSi_2 contacts *IEEE J. Quantum Electron.* **22** 1073–7
- [6] Chan P T, Choy H S, Shu C and Hsu C C 1995 High-performance InP/Ga_{0.47}In_{0.53}As/InP metal–semiconductor–metal photodetectors with a strained Al_{0.1}In_{0.9}P barrier enhancement layer *Appl. Phys. Lett.* **67** 1715–7

- [7] Wohlmuth W A, Arafa M, Mahajan A, Fay P and Adesida I 1996 InGaAs metal–semiconductor–metal photodetectors with engineered Schottky barrier heights *Appl. Phys. Lett.* **69** 3578–80
- [8] Martin M A, Song K C, Robinson B J, Simmons J G, Thompson D A and Gouin F 1996 Very low dark current InGaP/GaAs MSM-photodetector using semi-transparent and opaque contacts *Electron. Lett.* **32** 766–7
- [9] Aboudou A, Vilcot J P, Decoster D, Chenoufi A, Delhaye E, Boissenot P, Varin C, Deschamps F and Lecuru I 1991 Ultralow dark current GaAlAs/GaAs MSM photodetector *Electron. Lett.* **27** 793–6
- [10] Wohlmuth W A, Fay P and Adesida I 1996 Dark current suppression in GaAs metal–semiconductor–metal photodetectors *IEEE Photon. Technol. Lett.* **8** 1061–3
- [11] Lee C T, Lan M H and Tsai C D 1997 Improved performances of InGaP Schottky contact with Ti/Pt/Au metals and MSM photodetectors by $(\text{NH}_4)_2\text{S}_x$ treatment *Solid-State Electron.* **41** 1715–9
- [12] Seo J W, Caneau C, Bhat R and Adesida I 1993 Application of indium-tin-oxide with improved transmittance at $1.3 \mu\text{m}$ for MSM photodetectors *IEEE Photon. Technol. Lett.* **5** 1313–5
- [13] Strittmatter A, Kollakowski S, Dröge E, Böttcher E H and Bimberg D 1996 High speed, high efficiency resonant-cavity enhanced InGaAs MSM photodetectors *Electron. Lett.* **32** 1231–2
- [14] Kim J H, Griem H T, Friedman R A, Chan E Y and Ray S 1992 High-performance back-illuminated InGaAs/InAlAs MSM photodetector with a record responsivity of 0.96 A/W *IEEE Photon. Technol. Lett.* **4** 1241–4
- [15] Yuang R H, Chyi J I, Chan Y J, Lin W and Tu K Y 1995 High-responsivity InGaAs MSM photodetectors with semi-transparent Schottky contacts *IEEE Photon. Technol. Lett.* **7** 1333–5
- [16] Lin S D and Lee C P 2001 Hole Schottky enhancement and its application to metal–semiconductor–metal photodetectors *J. Appl. Phys.* **90** 5666–9
- [17] Sze S M, Coleman D J, Loya J R and Loya A 1971 Current transport in metal–semiconductor–metal (MSM) structures *Solid-State Electron.* **14** 1209–18
- [18] Sze S M 1981 *Physics of Semiconductor Devices* 2nd edn (New York: Wiley)
- [19] Sadwick L P, Kim C W, Tan K L and Streit D C 1991 Schottky barrier heights of n-type and p-type $\text{Al}_{0.48}\text{In}_{0.52}\text{As}$ *IEEE Electron. Device Lett.* **12** 626–8
- [20] Shannon J M 1976 Control of Schottky barrier height using highly doped surface layers *Solid-State Electron.* **19** 537–43
- [21] Chuang S L 1995 *Physics of Optoelectronic Devices* (New York: Wiley)
- [22] Zouganeli P, Stevens P J, Atkinson D and Parry G 1995 Design trade-offs and evaluation of the performance attainable by GaAs- $\text{Al}_{0.3}\text{Ga}_{0.7}\text{As}$ asymmetric Fabry-Perot modulators *IEEE J. Quantum Electron.* **31** 927–43